Communication-aware Restoration of Smart Distribution Grids Based on Optimal Allocation of Resilience Resources

Youba Nait-Belaid, Yiping Fang, Zhiguo Zeng, Patrick Coudray, and Anne Barros

Abstract—**Although power grids have become safer with increased situational awareness, major extreme events still pose reliability and resilience challenges, primarily at the distribution level, due to increased vulnerabilities and limited recovery resources. Information and communication technologies (ICTs) have introduced new vulnerabilities that have been widely investigated in previous studies. These vulnerabilities include remote device failures, communication channel disturbances, and cyber-attacks. However, only few studies have explored the opportunity offered by communications to improve the resilience of power grids and eliminate the notion that power-telecom interdependencies always pose a threat. This paper proposes a communication-aware restoration approach of smart distribution grids, which leverages power-telecom interdependencies to determine the optimal restoration strategies. The states of grid-energized telecom points are tracked to provide the best restoration actions, which are enabled through the resilience resources of repair, manual switching, remote reconfiguration, and distributed generators. As the telecom network coordinates the allocation of these resilience resources based on their coupling tendencies, different telecom architectures have been introduced to investigate the contribution of private and public ICTs to grid management and restoration operations. System restoration uses the configuration that follows a remote fast response as the input to formulate the problem as mixed-integer linear programming. Results from numerical simulations reveal an enhanced restoration process derived from telecom-aware recovery and the co-optimization of resilience resources. The existing disparity between overhead and underground power line configurations is also quantified.**

Index Terms—**Smart grid, smart distribution grid, distribution system restoration, cyber-physical system, resilience, co-optimization, information and communication technology (ICT), mixed-integer linear programming (MILP).**

Manuscript received: January 3, 2024; revised: May 1, 2024; accepted: September 3, 2024. Date of CrossCheck: September 3, 2024. Date of online publication: October 4, 2024.

This work was supported by EDF/Orange/SNCF in the framework of the Chair on Risk and Resilience of Complex Systems (CentraleSupelec, EDF, Orange, SNCF).

Y. N. Belaid (corresponding author), Y. Fang, Z. Zeng, and A. Barros are with CentraleSupélec, University of Paris-Saclay, Paris, France, and Y. N. Belaid is also with Electricité de France (EDF) R&D, Paris, France (e-mail: youba.nait-belaid@centralesupelec.fr; yiping.fang@centralesupelec.fr; zhiguo.zeng@centralesupelec.fr; anne.barros@centralesupelec.fr).

P. Coudray is with Electricité de France (EDF) R&D, Paris, France (e-mail: patrick.coudray@edf.fr).

DOI: 10.35833/MPCE.2024.000015

NOMENCLATURE

A. Sets

C	Set of crews
CD, CD^{dp}	Set of candidate nodes to receive a distributed generator (DG) and set of nodes that DG placement crews visit (candidate nodes and depots)
DP	Set of depots
F	Set of damaged power lines
F^o, F^u	Sets of damaged overhead and underground lines
F^{dp}	Set of nodes of damaged lines and depots
GC	Set of DG placement crews
L, L^u	Sets of all lines and underground lines
L^{ar}, L^{cb}	Sets of auto-reclosing and circuit-breaking lines
L^m, L^r	Sets of manual and remote switchable lines
N	Set of all power nodes
$n(j)$	Set of neighbor nodes of node j
$n_m(l)$	Set of neighbor manual lines of line l
RC, MC	Sets of repair and manual switching crews
S	Set of high-voltage (HV)/medium-voltage (MV) substations (SSs)
U	Set of utility-owned access points
X, W	Sets of fixed and wireless access points

B. Parameters

α, β, γ	Weighting coefficients
$C_i^{ns}, C_i^{sw}, C_i^{rc}, C_i^{mc}, C_i^{gc}$	Non-supplied load, switching, repair, manual-switching, and DG placement costs
$\lvert C \rvert$	Number of crews
$E_i^{\max}$	The maximum energy storage of battery at node i
f_i	Binary parameter that equals 1 if telecom point i fails, and 0 otherwise

$\lvert F^{dp} \rvert$	Number of nodes (damaged lines and depots)
GT_g	DG placement time at bus g
M	Large number
p_i^{disc}	Active battery discharging power of node i
$P^{\max}, Q^{\max}, S^{\max}$	Total active, reactive, and apparent power demands
$P^{dg,\max}, Q^{dg,\max}$	The maximum active and reactive DG power
r_{ij}, x_{ij}	Resistance and reactance of line (i,j)
Res_l	Demand of repair resource from faulted line l
Res^{dp}	Repair resource available at depot dp
RT_l, MT_l	Repair time and manual switching time of faulted line l
s_i	Binary parameter that equals 1 if i is an SS, and 0 otherwise
$\lvert T \rvert$	Number of restoration time steps
TT_{lm}	Travel time from l to m (depot, line, or bus)

C. Variables

$a_{ij,t}$	1 if line $l=(i,j)$ is available at time t, and 0 otherwise
$a_{i,t}^e$	1 if bus i is available at time t, and 0 otherwise
$a_{i,t}^{dg}$	1 if a DG is available at bus i at time t, and 0 otherwise
AT_l^k	Arrival time of crew k to damaged line l
$b_{i,t}$	1 if battery at bus i is not empty at time t, and 0 otherwise
$c_{l,m}^k, c_l^k$	Binary variables describing crew k traveling from l to m and crew k visiting l
$d_{ij,t}$	1 if power flows on line $l=(i,j)$ at time t, and 0 otherwise
$E_{i,t}$	Energy storage of battery at node i at time t
$gc_{n,t}^{dp,k}$	1 if bus n is under DG-placement by crew k of depot dp at time t, and 0 otherwise
$mc_{l,t}^{dp,k}$	1 if line l is under manual switching by crew k of depot dp at time t, and 0 otherwise
$sw_{l,t}$	1 if switch on line $l=(i,j)$ is closed at time t, and 0 otherwise
$p_{ij,t}, q_{ij,t}$	Active and reactive power flows of line $l=(i,j)$ at time t
$p_{i,t}^{ns}, q_{i,t}^{ns}$	Losses of active and reactive loads at node i at time t
$p_{i,t}^{dg}, q_{i,t}^{dg}$	Active and reactive DG power at node i at time t
$rc_{l,t}^{dp,k}$	1 if line l is under repair by crew k of depot dp at time t, and 0 otherwise
$ss_{i,t}^c$	1 if the telecom service of an SS i is available at time t, and 0 otherwise
$sw_{ij,t}$	1 if directed switch on line $l=(i,j)$ is closed at time t, and 0 otherwise
$T_{i,t}^c$	1 if the telecom service from operator's access point i is available at time t, and 0 otherwise
$T_{i,t}^e$	1 if electricity supply for operator's access point i is available at time t, and 0 otherwise
$u_{i,t}^c$	1 if telecom service from utility-owned access point i is available at time t, and 0 otherwise
$v_{i,t}$	Voltage magnitude at node i at time t
$w_{i,t}, w_{i,t}^1$	Linearization binary variables
$y_{i,t}^e$	1 if bus i is energized at time t, and 0 otherwise
$y_{i,t}^{dg}$	1 if a DG is connected at bus i at time t, and 0 otherwise

D. Vectors

$\boldsymbol{a}$	Vector of availabilities of power buses, lines, or DGs
$\boldsymbol{c}$	Vector of all intervention crews
$\boldsymbol{d}$	Vector of power flow directions
$\boldsymbol{E}$	Vector of state-of-charge and depletion status of batteries
$\boldsymbol{p}$	Vector of electrical quantities (active/reactive power and node voltages)
$\boldsymbol{sw}$	Vector of switch statuses
$\boldsymbol{T}$	Vector of electrical and telecom statuses of all telecom points
$\boldsymbol{w}$	Vector of linearization variables
$\boldsymbol{y}$	Vector of connectivities of buses to power grid or DGs

I. Introduction

In the face of adversity posed by extreme events such as natural disasters, cyber-physical intrusions, and human errors, smart grids adhere to stringent standards of supply quality and service continuity. As a result, all stakeholders are committed to enhancing the reliability and resilience of the power grid [1]. Resilience is a multi-faceted concept that includes proactive planning, robustness, damage evaluation, and grid restoration [2], [3]. In contrast to the cost-prohibitive hardening measures [1], [4], operational interventions during the restoration phase present significant potential for bolstering resilience. This involves restoring the power grid to an acceptable level of functionality as swiftly and with as little societal disruption as possible. The methodologies for achieving this goal have advanced from rule-based expert systems to heuristic approaches (including genetic algorithms and fuzzy logic), mathematical optimization, and the application of artificial intelligence (AI) techniques [3], [5].

Recent studies have introduced resilience-based optimization for grid restoration. Given their pivotal role, transmission networks have been at the forefront of these endeavors, serving as the backbone of power grids [6], [7]. Nevertheless, the proliferation of grid-integrated applications such as renewable energy sources, electric vehicles, and smart meters, along with the widespread adoption of information and communication technologies (ICTs) and the intrinsic susceptibilities of smart distribution grids (SDGs), has necessitated rigorous examinations of restoration optimization at the distribution level [8]. Therefore, even if the insights from the present research can be effectively applied to transmission grids and other industrial cyber-physical systems, this paper focuses on smart distribution grids by considering advanced operational aspects of radiality, switching, and power balancing.

Current approaches for distribution system restoration (DSR) have ranged from single-resource optimization in the power grid to multi-resource co-optimization in interdependent systems. Investigated resources have primarily included reconfiguration switches, intervention crews, and mobile power storage. Reference [4] focused on the fast response of the power grid using remotely controlled switches (RCSs). A unified two-stage optimization model was constructed, starting from proactive RCS allocation and followed by remote reconfiguration. A two-stage remote and manual switching was considered in [9], where an initial mixed-integer linear programming (MILP) formulation describes feeder reconfigurations with DG-assisted grid-forming, prior to a similar optimization approach being used to find the optimal sequence of switching operations.

For multi-resource DSR optimization, [10] modeled the routing and scheduling of crews to disrupted components by using two MILPs corresponding to the cases of ① full-repair requirements prior to reconnection and ② possible partial operation. Some studies have considered dynamic programming [11], Markov decision processes [12], and reinforcement learning [13] as promising means of overcoming computation and scalability issues related to models of large-scale real-world power grids. However, mixed-integer programming (MIP) approaches have been predominantly used in the co-optimization of multiple resilience resources to achieve faster crew interventions with microgrid formation capabilities. Reference [14] coordinated the resilience strategies for repair crew (RC) dispatch, distributed generator (DG) placement, and reconfiguration. An MILP was formulated based on power flow, routing, and scheduling constraints to optimize the served load and the restoration time. Based on similar objectives and resources while using vertex-wise routing instead of the edge-wise approach, [15] constructed an MIP for optimal DSR in minimal time. The problem is convexified and linearized equivalently, then reduced by pre-assigning damage and DG candidates to depots. The co-optimization approach was extended in [16] to encompass damage assessment for a comprehensive DSR analysis. The designed framework brings crew schedules and reconfiguration to the damage assessment stage, resulting in a dynamic update of the restoration schedules as failures are revealed. All these recent contributions to DSR analysis are comprehensive and address many aspects related to restoration modeling for single- and multi-resource problems with various constraints and scalability issues. However, none of them have considered the omnipresent power-telecom interdependencies.

DSR invokes many power-telecom interdependent functions from outage management and wide-area monitoring, protection, and control systems, e. g., volt/var control, fault location, isolation, and service restoration (FLISR), and intervention workforce management [4], [17], [18]. According to [19], these power-telecom interdependencies can be seized by extending the optimal power flow model to include the information flow. Due to prevailing event-driven communications, the resulting integrated model is nonconvex and highly nonlinear. A similar complexity was observed in [20], wherein a cyber-constrained power flow model was developed to evaluate and enhance power grid resilience, then a bi-level linear programming exact reformulation was used to solve the problem. Reference [21] investigated the status of the telecom service (TS) by coordinating repair and reconfiguration alongside the deployment of emergency communications. However, the power supply effect on feeder terminal units (FTUs) is considered only before the batteries were depleted, without prioritizing the recovery of nodes from which FTUs were initially supplied. An emergency deployment of communication systems was initiated, considering solely the impact of telecommunications on the power grid, while the reciprocal influence of the power grid on communication networks was set aside. Reference [22] presented a fine-grained description of the power-telecom interdependencies using a discrete-event evaluation methodology. However, backup power supplies such as batteries in communication devices were not modeled, making the analysis of the impact on the restoration process incomplete. The recent study in [23] quantified the effects of power supply reliability on the backup time of a 5G base station, with the goal of establishing situational awareness of the ability of base station backup energy to participate in emergency power supply to the distribution grid. However, the considered approach did not model the dependency of the power grid on the telecom service from 5G base stations.

These cutting-edge studies have considered one-way or no power dependence on communications, effectively narrowing the scope of the telecom network to its cyber layer alone. By contrast, practical evidence strongly demonstrates the importance of the physical layer of a telecom network, which can be affected by either physical damage or a shortage in the power supply [24]. In addition, no previous DSR contribution has considered underground lines, which differ from overhead lines in terms of failure isolation [25]. To bridge these gaps, this paper considers both the cyber and physical layers of the telecom network, allowing to capture two-way power-telecom interdependencies: the distribution grids depend on telecom networks to control switches and communicate with intervention crews, whereas telecom assets depend on the power supply from the distribution grid or backup batteries to maintain the operating state. A telecom-aware co-optimization is utilized to solve the DSR problem, with novel contributions outlined as follows.

1) The proposed restoration approach adeptly encapsulates the bidirectional interdependencies between power and telecommunications, along with the intricate coupling among restoration resources and the dynamics within the public-private telecom sectors.

2) A co-optimization is formulated to seek the optimal DSR strategies by leveraging the information on the availability of telecom assets and their power supply.

3) Various grid architectures are considered by the two broad families of overhead and underground lines, demonstrating the minimal model changes for configuration evolution.

4) A simplified formulation is used for radiality conditions, and a realistic multi-feeder network is constructed to validate the proposed restoration approach.

The remainder of this paper is organized as follows. Section II introduces the system model and proposed restoration approach. Section III presents simulations and numerical results. Section IV provides the conclusion of this paper.

II. System Model and Proposed Restoration Approach

Distribution grids are meshed by design but operate radially to limit the propagation of faults by opening switches during normal operation (called tie switches). The term "failure" is used interchangeably with fault, damage, outage, and incident to indicate the unavailability of a component due to an exogenous event. Figure 1 summarizes the interactions between the intra- and inter-domain components under four main actions: power supply, TS, repair/isolation, and DG placement (where each arrow originates from an entity providing the action/service and ends at a targeted entity).

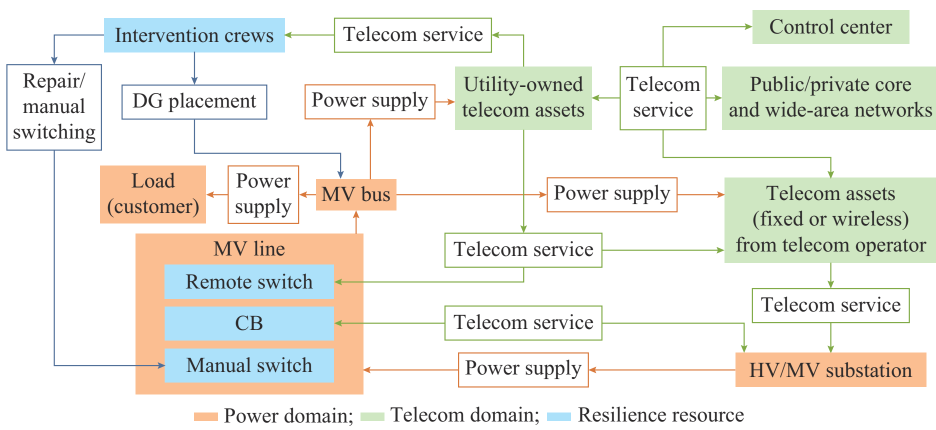

Fig. 1. Summarized interactions between intra- and inter-domain components.

Following the outbreak of an extreme event, the fast response reconfigures the network by maneuvering the RCSs, relying on prior knowledge about the structure and operation of the grid as well as monitoring information. The entire process is conducted within a few minutes of the surge and typically allows for a partial restoration. The fast response comprises three phases. ① Automatic isolation: circuit breakers (CBs) associated with the affected feeders are automatically opened to protect the high-voltage (HV)/medium-voltage (MV) substations (SSs). Some overhead feeders contain automatic circuit reclosers (ACRs) that can limit the affected zone. ② Remote isolation: the wide automatically isolated zone is reduced by opening RCSs. Data from fault detectors are used to localize failures and open RCSs wherever they allow the isolation of nodes from damaged zones. ③ Reconfiguration: the achieved isolation is leveraged to restore loads. The topological, power flow, and zone isolation conditions are verified prior to any reconfiguration of the network. Please refer to [4] and [9] for more details on the fast response.

Following the initial response, the SDG achieves a limited recovery that must be complemented by multiple resources: remote/manual switching, RCs/manual-switching crews (MCs), and DGs. An MILP formulation is proposed to co-optimize restoration resources, where the optimal combination of resilience resources, subject to topological, operational, and interdependency constraints, is sought. Co-optimization is motivated by the tight coupling of the considered resources. For instance, an intervention crew finishing a repair at a given line must inform the control center that the latter may execute a reconfiguration using switches before it commands the crew to reconnect the repaired segment. Similarly, microgrids formed using DGs combine the tasks achieved by specialized intervention crews and network reconfiguration by manual and remote switches. A complementarity also exists between the repair and placement of DGs, as zones that receive DGs can most likely afford the delayed repair, which allows other zones to be prioritized, and vice versa.

Inter-resource coupling is even more appealing when ICTs are recognized as vectors of coordination. Unlike the fast response, in which telecom points are affected only by direct failures, power shortages affect major telecom points after the depletion of batteries. Therefore, the DSR stage deals with bidirectional power-telecom interdependencies, where ICTs are dependent on the power grid for power supply, and the power grid is dependent on ICTs for controlling field assets and coordinating restoration strategies. The information provided to the DSR stage ($t=0$) includes remote reconfiguration from the first response and outage diagnoses. This is organized as a record of identified damages, estimation of travel/repair time, and indication of the accessibility of damaged sites.

A. Zone-separation Constraints

Three zones can be distinguished during an event.

1) Damaged zone: part of the grid where the initial failure occurs and that sustains subsequent damage due to failure propagation.

2) Out-of-service safe zone: part of the grid initially included in the damaged zone but that could be isolated from damage using switches. Elements in this zone wait for reconnection to the grid.

3) Supplied safe zone: part of the grid that is safe from damage and energized.

Figure 2 presents the fault propagation of two widely used topologies for overhead and underground lines, respectively. For overhead lines, only one switch is present at each line between two nodes (buses); thus, the tightest isolation can be achieved by opening the switches of neighboring lines. However, for underground lines, switches are often positioned on each side of a node, allowing for better isolation by opening both sides of the damaged line.

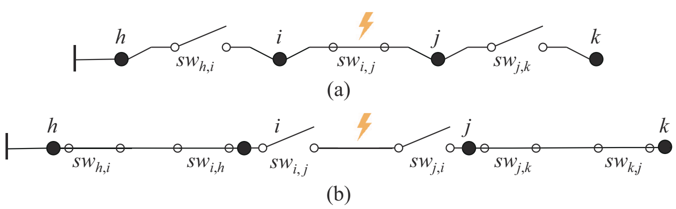

Fig. 2. Fault propagation of two widely used topologies for overhead and underground lines. (a) Overhead. (b) Underground.

$$a^e_{i,t}+sw_{l,t}-1\le a^e_{j,t}\quad \forall l=(i,j)\in L,\forall t \tag{1}$$

$$a^e_{i,t}\le a^e_{i,t-1}+a_{l,t}\quad \forall l=(i,j)\in F^o,\forall t \tag{2}$$

$$a^e_{i,t}\le a^e_{i,t-1}+a_{ij,t}+(1-sw_{ij,t})\quad \forall (i,j)\in F^u,\forall t \tag{3}$$

$$sw_{l,t}\le sw_{ij,t}\quad \forall l=(i,j)\in L^u,\forall t \tag{4}$$

$$sw_{l,t}\le sw_{ji,t}\quad \forall l=(i,j)\in L^u,\forall t \tag{5}$$

$$sw_{ij,t}+sw_{ji,t}-1\le sw_{l,t}\quad \forall l=(i,j)\in L^u,\forall t \tag{6}$$

Constraint (1) ensures that damaged zones are not connected to safe (supplied or out-of-service) zones. This is guaranteed by the requirement for open lines between safe and damaged zones. A connection between supplied and out-of-service zones is possible. From (2) and (3), a power bus can be restored if no neighboring overhead or underground line is damaged ($a_{ij,t}=0$) or if it is isolated from a neighboring underground line. The variable $sw_{ij,t}$ is directed because it represents the switch closest to node i, and $sw_{ji,t}$ is the switch closest to node j in underground lines. By contrast, the undirected variable $sw_{l,t}$ is used when direction is not required. Constraints (4)-(6) state that an underground line is closed only when both switches are closed and is open otherwise. Except for constraints (3)-(6), the undirected variable $sw_{l,t}$ is used throughout the model to represent the state of line $l=(i,j)$.

B. Radiality Constraints

A novel formulation is adopted to guarantee the radiality of the power grid:

$$d_{ij,t}+d_{ji,t}\le sw_{l,t}\quad \forall l=(i,j)\in L,\forall t \tag{7}$$

$$sw_{l,t}-(2-y^e_{i,t}-y^e_{j,t})\le d_{ij,t}+d_{ji,t}\quad \forall l=(i,j)\in L,\forall t \tag{8}$$

$$d_{ij,t}+d_{ji,t}-(2-y^e_{i,t}-y^e_{j,t})\le sw_{l,t}\quad \forall l=(i,j)\in L,\forall t \tag{9}$$

$$\sum_{\forall j\in n(i)} d_{ji,t}\le a^e_{i,t}-s_i-y^{dg}_{i,t}\quad \forall i\in N,\forall t \tag{10}$$

$$\sum_{\forall j\in n(i)} d_{ij,t}\le M\left(\sum_{\forall j\in n(i)} d_{ji,t}+s_i+y^{dg}_{i,t}\right)\quad \forall i\in N,\forall t \tag{11}$$

Constraint (7) imposes a unidirectional power flow while capturing the existence of unsupplied closed lines in damaged zones. This fact is missed in all the reviewed studies, as the equality sign in (7) would mean that energizing (de-energizing) a line is equivalent to closing (opening) it. Then, (8) and (9) state that for all t, a line out of the damaged zones is safely energized as soon as it is closed. Note that the damage in a line is represented by the failure of directly connected nodes, implying that both failed-open and failed-closed events can be considered.

Constraint (10) prohibits the power flow into HV/MV SSs or nodes with a DG source and indicates that any other bus has at most one parent node. If the parent node does not supply power to the considered node i, or i is neither an SS nor a DG, then no downstream flow is possible from node i, as encoded in (11). The placement of DGs to form islanded zones (or microgrids) is anticipated by (10), and the resulting topology is a spanning forest, similar to the case of a multi-SS power grid. This construction enables the formation of out-of-service islands.

C. Power Flow Constraints

The LinDistFlow model is used to represent the power flow for all loads.

$$\sum_{\forall j\in n(i)} p_{ij,t}+p^d_i=\sum_{\forall j\in n(i)} p_{ji,t}+p^{ns}_{i,t}+p^{dg}_{i,t}\quad \forall i\in N\backslash S,\forall t \tag{12}$$

$$\sum_{\forall j\in n(i)} q_{ij,t}+q^d_i=\sum_{\forall j\in n(i)} q_{ji,t}+q^{ns}_{i,t}+q^{dg}_{i,t}\quad \forall i\in N\backslash S,\forall t \tag{13}$$

$$-M(1-d_{ij,t})\le v_{i,t}-v_{j,t}-2(r_{ij}p_{ij,t}+x_{ij}q_{ij,t})\le M(1-d_{ij,t})\quad \forall (i,j)\in L,\forall t \tag{14}$$

$$0\le p_{ij,t}\le S^{\max}d_{ij,t}\quad \forall (i,j)\in L,\forall t \tag{15}$$

$$0\le q_{ij,t}\le S^{\max}d_{ij,t}\quad \forall (i,j)\in L,\forall t \tag{16}$$

$$v^{\min}_i\le v_{i,t}\le v^{\max}_i\quad \forall i\in N,\forall t \tag{17}$$

$$(1-y^e_{i,t})p^d_i\le p^{ns}_{i,t}\le p^d_i\quad \forall i\in N,\forall t \tag{18}$$

$$(1-y^e_{i,t})q^d_i\le q^{ns}_{i,t}\le q^d_i\quad \forall i\in N,\forall t \tag{19}$$

$$0\le p^{dg}_{i,t}\le P^{dg,\max}y^{dg}_{i,t}\quad \forall i\in D,\forall t \tag{20}$$

$$0\le q^{dg}_{i,t}\le Q^{dg,\max}y^{dg}_{i,t}\quad \forall i\in D,\forall t \tag{21}$$

Constraints (12) and (13) express the power balance of each bus. The difference in the node voltages is given in (14) in terms of power and impedance quantities ($v_{i,t}$ is used here for linearization purposes, as it is the square of the actual node voltage). Constraints (15) and (16) limit the power capacity of closed lines, whereas (17) bounds the bus voltage. Unsupplied power is restrained by (18) and (19).

D. Telecom Constraints

Grid operators use public and/or private communications for DSR and other grid applications [26]-[28]. Public ICTs range from wired (fiber-optic, copper: PSTN, xDSL) to licensed (GSM, CDMA, LTE, 5G, etc.) and unlicensed (WiFi, LoRa, SigFox, etc.) wireless technologies [29].

Distribution system operators (DSOs) subcontract telecom operators to provide and manage the access and core infrastructure that enable SSs, field devices, and crews to connect to the control center and other central functions (DSO datacenters, procurement centers, billing systems, etc.). This subcontracting relationship has the advantages of reduced operational costs, wide coverage, and specialized support from experienced telecom teams. An alternative is to deploy a private network managed by a DSO to cope with privacy and congestion issues in public ICTs. Unfortunately, this imposes limitations such as a narrow bandwidth (i. e., reduced data rate), high operating expense (OPEX), niche technology, and very restricted ecosystem. These technologies encompass power line communications (PLCs), for which the DSO already has the basic infrastructure and private mobile radio (PMR) communications, operating in a dedicated frequency band.

A hybrid setting can be a good compromise between the advantages and disadvantages of public and private communications, where great flexibility exists for selecting a technology that meets the requirements of a given grid application [26]. The constraints described provide an example of a hybrid architecture that can be captured by the proposed restoration approach, where a utility-owned ICT infrastructure is combined with telecom operator services. The hierarchical setup of telecom networks is illustrated by a wide area network (WAN) and a core network that provide services to public and private access points (APs), which in turn serve as grid assets. Therefore, in addition to connecting the RCSs, crews, and SSs, other communication components are modeled as follows.

1) Private or utility-owned APs (U-APs): these are major DSO assets equipped with large batteries. Each U-AP has a primary fixed (wired) link and a secondary wireless link in the case of a hybrid configuration. U-APs can provide RCSs and intervention crews with the requested TSs.

2) Telecom operator fixed APs (F-APs): these serve DSO assets (HV/MV SS and RCSs) in a public configuration, and can be a primary link for U-APs in a hybrid configuration. The battery can last for several hours.

3) Telecom operator wireless APs (W-APs): these serve the DSO assets (HV/MV SS and RCSs) in a public configuration and can be a secondary link for U-APs in a hybrid configuration. The battery can last for several hours.

The upper layer that serves the APs is called the core network, which collects, processes, and transmits data through technology-dependent aggregation points, location registers, and gateways. Some requests can be routed directly at the core level, whereas in the case of DSR, other requests resort to the central functions of power grid such as the control center. The core network connects to the WAN of the utility, which is a collection of routers, switches (communication switches), and various networking equipment that grant access to grid functions and applications. The criticality associated with WANs has caused most power operators to deploy their own networks, which may or may not be handed over to a tier telecom operator for management [27]. In this paper, the core network and WAN are assumed to operate perfectly to concentrate on the effects of more vulnerable APs [30].

$$\frac{1}{M}\left(T_{k,t}^{c}+\sum_{\forall j:(j,i)\in W\times S}T_{j,t}^{c}\right)\leq ss_{i,t}^{c}\leq T_{k,t}^{c}+\sum_{\forall j:(j,i)\in W\times S}T_{j,t}^{c}\quad \forall (k,i)\in X\times S,\forall t \tag{22}$$

$$\frac{1}{M}\left(T_{k,t}^{c}+\sum_{\forall j:(j,i)\in W}T_{j,t}^{c}\right)\leq u_{i,t}^{c}\leq T_{k,t}^{c}+\sum_{\forall j:(j,i)\in W\times U}T_{j,t}^{c}\quad \forall (k,i)\in X\times U,\forall t \tag{23}$$

$$T_{i,t}^{c}\leq T_{i,t}^{e}\quad \forall i\in W\bigcup X,\forall t \tag{24}$$

$$\frac{1}{M}(1-f_i)(E_{i,t}+y_{i,t}^{e})\leq T_{i,t}^{e}\leq M(1-f_i)(E_{i,t}+y_{i,t}^{e})\quad \forall i\in W\bigcup X,\forall t \tag{25}$$

$$\frac{1}{M}E_{i,t}\leq b_{i,t}\leq E_{i,t}\quad \forall i\in W\bigcup X,\forall t \tag{26}$$

$$E_i^{\min}\leq E_{i,t}\leq E_i^{\max}\quad \forall i\in W\bigcup X,\forall t \tag{27}$$

$$E_{i,t}=E_{i,t-1}-p_i^{disc}(1-y_{i,t-1}^{e})b_{i,t-1}\quad \forall i\in W\bigcup X,\forall t \tag{28}$$

The cross sign between different sets is used to represent the indexed sets in which only meaningful elements are evaluated. In other words, $W\times S$ does not contain all possible two-dimensional (j,i) combinations formed by the elements of the two sets but includes only the valid pairs formed by an SS $i\in S$ connected to a W-AP $j\in W$.

In (22), the summation over all W-APs associated with SS i shows the redundancy offered by W-APs, which is not found in fixed networks (dedicated wired links). The TS available to an HV/MV SS depends on the availability of either an F-AP or a secondary W-AP. Although common, this is a generic choice for connecting SSs, and (22) is easily adaptable to other technologies. A hybrid public/private telecom architecture in which private assets eventually send and receive data through public networks is expressed in (23). Constraints (24) and (25) emphasize that the TS is available only when the power supply is guaranteed by the power grid or backup batteries. In this case, the HV/MV SSs and U-APs will not necessarily fail but will operate in blind mode.

In (26), the binary variable $b_{i,t}$ is linked to $E_{i,t}$ to indicate whether the battery of the AP i is empty ($b_{i,t}=0$). Equation (27) binds the state-of-charge (SoC) of the battery using the minimum and maximum capacities. The battery discharge, as in (28), includes power p_i^{disc} and has a quadratic component $y_{i,t}^{e}b_{i,t}$, which is easily linearized using a binary variable $w_{i,t}^{1}$ (product of two binary variables).

E. Routing and Scheduling Constraints

Damage assessment is conducted by diagnostic crews, helicopter-transport teams, and aerial drones [8], with the purpose of data collection and the precise identification of damage sites. This process is instrumental in estimating key parameters such as repair durations, travelling time, and the necessary allocation of resources. The DSO exploits the gathered information to organize operations by allocating resources and providing timelines and travel paths. This is described by the well-known routing and scheduling problem [31]. For the DSR problem, the depots and damaged lines are the nodes connected with road paths that are seen as edges, and the aim is to determine the sequence of locations for each crew to visit while minimizing the overall restoration time. The vehicle routing problem (VRP) has been adopted in many recent studies [14], [16] to model the dispatch of RCs and/or DG placement. Given that tasks such as manual switching, repairs, and DG placement are executed at the sites of damage, and considering the interdependencies between intervention crews, ICTs, and switches at these nodes, the edge-centric approach traditionally used in the VRP is less suitable for addressing the complexities of the DSR problem.

We adopt the node-centered approach proposed and demonstrated in [15] to bypass the issues of transportation-grid coupling and their different timescales. Let c be a binary variable representing a crew k visiting node l at time t. Specifically, $c=rc$ represents an RC, $c=mc$ represents an MC, and $c=gc$ represents a DG placement crew (labeled as GC). Variable $c^k_{l,t}$ provides the same information in the present model as $c^k_{l,m}$, c^k_l, and AT^k_l used in [14] and [16]. Still, the number of variables is comparable between $c^k_{l,t}$ with $|C||F^{dp}||T|$ elements and the edge-centered approach that necessitates $|C||F^{dp}|^2+|C||F^{dp}|$ elements. The squared term indicates that the edge-centered approach grows fast with an increase in the handled failures, whereas the node-centered approach grows slower with the number of damages, and depends on the number of time steps that is usually limited by other parts of the global model. The form $c^k_{l,t}$ from [15] is extended here to $c^{dp,k}_{l,t}$ to indicate that each crew k is linked to a given depot dp and to integrate the widely used problem reduction techniques that pre-assign damage and DG candidates to depots [14], [15].

$$\sum_{\tau=0}^{\min(TT^c_{l,m},T-t)} (c^{dp,k}_{l,t+\tau}+c^{dp,k}_{m,t}-1)\leq 0 \quad \forall l\neq m, \forall(dp,k,l,m)\in DP\times C\times F^{dp}\times F^{dp}, C=RC\cup MC, \forall t \tag{29}$$

$$\sum_{\tau=t}^{T}\sum_{\forall(dp,k)\in DP\times RC} mc^{dp,k}_{l,\tau}\leq M\left(1-\sum_{\forall(dp,k)\in DP\times RC} rc^{dp,k}_{l,t}\right) \tag{30}$$

$$\begin{cases} a_{l,t}\leq \dfrac{\sum_{\tau=0}^{t} h(\tau)}{RT_l+2\sum_{\forall m\in n_m(l)} MT_m} \quad \forall l\in F, \forall t \\ h(t)=\sum_{\forall(dp,k)\in DP\times RC} rc^{dp,k}_{l,t}+\sum_{\forall(dp,k)\in DP\times MC} mc^{dp,k}_{l,t} \end{cases} \tag{31}$$

$$\sum_{\forall l\in F} a_{l,T}\cdot Res_l\leq Res^{dp} \quad \forall(dp,l)\in DP\times F \tag{32}$$

$$h(t)+a_{l,t}\leq 1 \quad \forall l\in F, \forall t \tag{33}$$

According to (29), a crew is at a maximum of one node (a damaged line or depot) at any given t, and traveling time of at least TT^{rc}_{lm} and TT^{mc}_{lm} would be required for an RC and MC, respectively, to go from l to m. From (30), no isolation crew can visit an incident $l\in F$ at any t after being visited by an RC. Constraint (31) shows that a line is repaired when an RC and MC spend sufficient time at the node, starting with MT_l to manually isolate the damaged site and then RT_l for the repair, before spending MT_l in reconnecting the restored line. RCs can perform manual switching. A depot can handle only a limited amount of damage (32). In (33), the damaged line is in one of the four following states at any time step: not yet visited, in isolation, under repair, or resolved.

$$\sum_{\tau=0}^{\min(TT^{gc}_{m,0}+TT^{gc}_{n,0},T-t)} (gc^{dp,k}_{m,t+\tau}+gc^{dp,k}_{n,t}-1)\leq 0 \quad \forall n\neq m, \forall(dp,k,m,n)\in DP\times GC\times CD^{dp}\times CD^{dp}, \forall t \tag{34}$$

$$\sum_{\forall\tau=0}^{t}\sum_{\forall n\in CD} gc^{dp,k}_{n,t}\leq \sum_{\forall\tau=0}^{t} gc^{dp,k}_{0,t} \quad \forall(dp,k,n)\in DP\times GC\times CD \tag{35}$$

$$a^{dg}_{n,t}\leq \frac{1}{GT_n}\sum_{\tau=0}^{t}\sum_{\forall(dp,k)\in DP\times GC} gc^{dp,k}_{n,\tau} \quad \forall n\in CD, \forall t \tag{36}$$

$$\sum_{\forall(dp,k)\in DP\times GC} gc^{dp,k}_{n,t}+a^{dg}_{n,t}\leq 1 \quad \forall n\in CD, \forall t \tag{37}$$

Unlike the routing of RCs and MCs, GCs must return to the depot after completing each task. This is based on the assumption that the considered DGs are truck-mounted and bulky, requiring an entire team for transport and installation. In (34), a crew is at a maximum of one node (a DG candidate or depot) at any given time t. The traveling time of at least $TT^{gc}_{n,0}$ is required between a node n and its depot (0 is used to indicate that a crew is returning from or heading to its depot). Constraint (35) enforces that no direct paths between the DG candidates are allowed. A DG is placed after a crew spends at least a placement time GT_n at a site n, as indicated in (36). From (37), a candidate node either has yet to be visited, is undergoing DG placement, or has a DG installed.

F. Interdependency Constraints

The first power-telecom dependence is revealed in (24) as the power grid energizes APs, making the TS available only when the physical equipment is up and running. Executing commands received by power grid assets presents another power-telecom dependence, where the power flow is regulated by the applied controls.

$$a_{l,t}\leq u_{k,t} \quad \forall(k,l)\in U\times L, \forall t \tag{38}$$

$$sw_{l,t-1}-u^c_{k,t}(2-a^e_{i,t}-a^e_{j,t})\leq sw_{l,t}\leq sw_{l,t-1}+u^c_{k,t}a^e_{i,t} \quad \forall l=(i,j)\in L^r\cup L^{ar}, (k,(i,j))\in U\times L, \forall t \tag{39}$$

$$sw_{l,t-1}\leq sw_{l,t}\leq sw_{l,t-1}+ss^c_{k,t}a^e_{i,t} \quad \forall l=(i,j)\in L^{cb}, (k,(i,j))\in S\times L, \forall t \tag{40}$$

Before switching, a line must be available for connection, which is conditioned in (38) by the status of the communication AP. Constraint (39) implies the dependence of RCSs and ACRs on TSs from U-APs. From (40), a CB operates only when TSs from an SS are available. The nonlinear square terms in (39) and (40) are easily linearized.

$$\begin{cases} sw_{m,t-1}-\varepsilon-z\le sw_{m,t}\le a_{l,t}+2-\varepsilon-z \quad \forall l\in F, \forall t \\ z=\left(1+\sum\limits_{\tau=1}^{t-1}h(\tau)\right)\Big/\left(1+\sum\limits_{\forall m\in n_M(l)}MT_m\right) \end{cases} \tag{41}$$

The interdependencies are also manifested between resilience resources. Constraints (31) and (36) already express that a line and DG are not operable unless the missioned crews have completed their tasks. In addition, the closest manual lines are first opened for the best isolation and then closed after task completion (41). The dependence of U-APs on public ICTs is represented in (23), which can be expanded to model other dependencies based on chosen hybrid architectures.

For applicability to DSR, such as the exchange of assets and real-time data on the state of mutually supplying nodes, this interdependency analysis requires close collaboration between power and telecom operators [32]. In addition to improving utility restoration operations, the proposed restoration approach can inform continuous inter-operability standardization efforts within international bodies [33], [34].

G. Objective Function

During an extreme event, it is the primary goal of a utility to recover power supply as quickly as possible to the maximum number of clients. In this paper, supplied power (or, conversely, unsupplied power) is adopted as a performance measure and used in the objective function of the formulated MILP problem. This is in addition to costs related to deployed resilience resources.

$$\begin{cases} \min\limits_{\boldsymbol{p},\boldsymbol{d},\boldsymbol{sw},\boldsymbol{c},\boldsymbol{a},\boldsymbol{y},\boldsymbol{T},\boldsymbol{E},\boldsymbol{w}}\Bigg[\alpha\sum\limits_{\forall t}\sum\limits_{\forall i\in N\setminus S}C_i^{ns}p_{i,t}^{ns}+\beta\sum\limits_{\forall t}\sum\limits_{\forall l\in L}C^{sw}w_{l,t}+\gamma\cdot \\ \left(\sum\limits_{\forall(dp,k,l,t)}C_i^{rc}\cdot rc_{l,t}^{dp,k}+\sum\limits_{\forall(dp,k,l,t)}C_i^{mc}\cdot mc_{l,t}^{dp,k}+\sum\limits_{\forall(dp,k,n,t)}C_i^{gc}\cdot gc_{n,t}^{dp,k}\right)\Bigg] \\ \text{s.t. (1)-(41), (43), (44)} \end{cases} \tag{42}$$

DSOs do not spare restoration efforts because of pressure from governments, regulatory bodies, public opinion, and operator commitment. Thus, the weighting coefficients are interrelated such that $\alpha\gg\beta$ and $\alpha\gg\gamma$, meaning that costs are only significant in cases of equivalent performance of restoration strategies. Switching costs are introduced because no change in the configuration is desired unless there is a gain in the restored power or damage isolation. C^{sw} is considered the same for all operated switches, and a binary variable $w_{l,t}$ is introduced for the linearization of $\left|sw_{l,t}-sw_{l,t-1}\right|$.

$$sw_{l,t}-sw_{l,t-1}\le w_{l,t} \quad \forall l\in L, \forall t \tag{43}$$

$$sw_{l,t-1}-sw_{l,t}\le w_{l,t} \quad \forall l\in L, \forall t \tag{44}$$

where $\left|sw_{l,t}-sw_{l,t-1}\right|$ equals 1 if the switch at line l is toggled (opened or closed) at t; otherwise, it equals 0.

III. Simulations and Results

Multi-feeder systems are constructed to validate the proposed restoration approach. Per-phase analysis is run in 20 kV balanced grids. We set $\alpha=10$, $\beta=0.1$, $\gamma=0.1$, $C_i^{ns}=0.5$, $C_i^e=1$, $C_i^{sw}=0.1$, $C_i^{rc}=3$, $C_i^{mc}=1$, and $C_i^{gc}=1.5$. The model is implemented in Pyomo and solved using CPLEX on a computer with an Intel Core i7 (2.5 GHz) and 32 GB of RAM.

A. DSR in a 36-bus System

Figure 3 shows a 36-bus system with a total demand of 1305 kW and service telecom points, where U_1-U_3 represent U-APs; nodes SS_1, SS_2, and SS_3 denote the HV/MV SSs; and the remaining nodes are the MV buses energizing the power loads, namely F-APs (X_1 and X_2) and W-APs (W_1 and W_2). The buses supplied by each feeder have a supply path from the associated SS (through green lines) and tie switches (dashed dark lines) to form inter-connections between the feeders. This is the nominal configuration from the grid planning stage, which is beyond the scope of this paper. We consider two configurations: full overhead (all lines are overhead) and hybrid overhead-underground (some lines are underground). Table I summarizes the types of sets and power lines, and delineates the underground lines used in the following analysis, where the number of overhead lines is kept higher to comply with the proportions in real distribution grids [25].

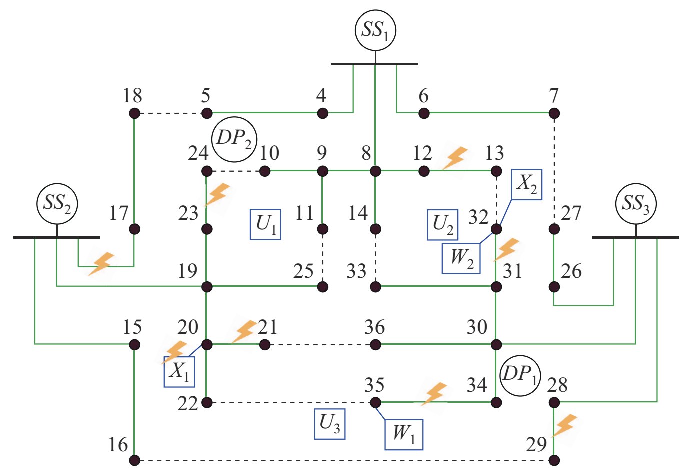

Fig. 3. 36-bus system with a total demand of 1305 kW and service telecom points.

TABLE I
Types of Sets and Power Lines

Set	Power line
L^{cb}	1-4, 1-6, 1-8, 2-15, 2-17, 2-19, 3-26, 3-28, 3-30
L^{ar}	19-20
L^{r}	8-9, 22-35, 20-22, 14-33, 23-24, 31-33, 12-13, 10-24, 5-18, 9-11, 11-25, 20-21, 4-5, 26-27, 30-31, 13-32, 7-27, 21-36, 19-23, 19-29
L^{m}	9-10, 30-34, 30-36, 6-7, 31-32, 17-18, 28-29, 8-12, 8-14, 34-35, 19-25, 15-16
L^{u}	1-6, 6-7, 9-10, 19-23, 23-24, 30-31, 31-32, 30-36

A scenario of eight instances of damage is considered, with seven affected power lines and one telecom AP (X_1 damaged during the entire period). Following the occurrence of events, the total supplied power drops from 100% in the initial phase to 29.5% after degradation, then increases with the RCS-based reconfiguration. As expected, the hybrid overhead-underground grids perform better than the full-overhead grids with 48.66% and 42.91% of the supplied power, respectively. Nevertheless, both cases are far from acceptable levels of restoration due to the limited improvement brought by remote switches. Thus, the distribution operators append other resources to subsequent restoration steps.

The resulting grid configuration is considered as the initial state ($t=0$) of the restoration process for which a time step of 1 hour is used. Under the distance-based optimization model described in [35], damages in Lines 2-17, 20-21, and 23-24 are pre-assigned to depot 1 (DP_1), with the remaining damage assigned to depot 2 (DP_2). Similarly, for safety, candidate buses for DG reception are set such that they are not directly connected to damaged lines, and then DP_1={36} and DP_2={14, 18, 22}. RCs, MCs, and GCs are initially located at the depots. DP_1 is set as $\{RC, MC, GC\}=\{2, 1, 1\}$, whereas DP_2 is $\{RC, MC, GC\}=\{2, 1, 1\}$. The travelling time is proportional to the distance between a depot and the damaged area or between two damaged areas, and MCs are twice as fast as RCs and GCs. Repair, manual-switching, and DG placement are selected for all lines for durations of two hours, one hour, and one hour, respectively. All crews depart from the depots. Without loss of generality, utility-owned APs are assumed to possess large batteries, whereas possible supply shortages can be experienced by public communications despite the battery storage duration being set to three hours in this instance. Damage to the telecom AP should be handled by the telecom operator, as the DSO repair strategy is limited to grid assets. The RCSs and intervention crews connect to the closest U-APs and CBs to their SSs. The U-APs and SSs are connected to the closest F-APs and W-APs.

A preliminary simulation is conducted to confirm the intuitive statement, which is well-verified in previous studies, that co-optimization achieves a better performance than non-cooperative approaches. Considering perfect communications (Case 1), we obtain a 12% gain in the total supplied load using the proposed co-optimization (as compared with the first case of separate optimization problems for reconfiguration and crew schedules [14]) and a 9% gain in a second case of co-optimization of the reconfiguration and RCs/MCs (without DGs).

Next, to quantify the criticality of TSs in the SDGs, a telecom-agnostic case is constructed (Case 2). This corresponds to a scenario in which restoration decisions are made without giving special attention to the status of telecom points. To accomplish this, the problem is solved first under perfect communications (Case 1). Then, the obtained solution of crew allocation (sequence of dispatching crews) is used as a parameter to solve the formulated problem for the remaining variables of telecom and switch states as well as power quantities. The proposed restoration approach, which leverages the state of the telecom points to find a restoration strategy, is referred to as telecom-aware (Case 3).

The evolution of the supplied power during the DSR stage in the three cases is shown in Fig. 4, where "O" and "U" describe the full-overhead and hybrid overhead-underground configurations, respectively. The co-optimization is solved within 1.25 s for Case 2 and 21 s for Case 3, respectively. Clearly, the hybrid configuration outperforms the purely overhead configuration in all three cases because of the advanced isolation capabilities of the underground networks. These results should be interpreted carefully, as the costs of manual switching and repair are assumed to be equal for underground and overhead networks in the conducted simulations, which may not be valid given that underground interventions are complex and time-consuming. Thus, tight isolation helps improve the level of restoration. However, the cost of introducing enhanced isolation should be considered in the future.

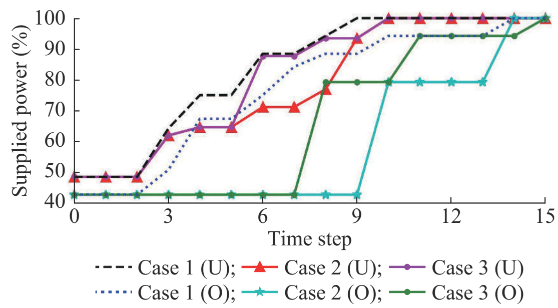

Fig. 4. Evolution of supplied power during DSR stage.

For the hybrid configuration, the ideal case of perfect communication achieves the best restoration compared with Cases 2 and 3 but can be described as overly optimistic because the ICTs are not perfect and undergo many failures. Cases 2 and 3 are more realistic because they include telecom failures, which are exploited in the proposed restoration approach (Case 3) to orient restoration choices and achieve a better recovery than that in Case 2, which does not link resource allocation to the state of telecom APs. A similar trend is observed in the overhead configuration. Here, the curve associated with Case 1 dominates the telecom-aware and telecom-agnostic cases, whereas the importance of prioritizing supply restoration to a few critical telecom points (which are useful for subsequent restoration) is demonstrated in Case 3, which outperforms Case 2.

Figure 5 shows the intervention crew schedules in Cases 2 and 3 for an overhead configuration. Unlike in Case 2, interventions related to Lines 30-31 and 34-35 are prioritized in Case 3, allowing earlier recovery of telecom points (X_2 and W_2) supplied by the buses involved. For instance, although the repairs of Lines 23-24 and 28-29 are completed at the 4$^{\text{th}}$ hour, their reconnection is delayed until the 8$^{\text{th}}$ hour in Fig. 5(b) when the TS is recovered. The MC 1 of DP_1 ($MC_{1,1}$) isolates Buses 32, 34, and 36 from the damaged Lines 30-31 by opening Buses 30-34, 30-36, and 31-32. This allows Buses 34 and 36 to be restored at the 8$^{\text{th}}$ hour following DG placements at Lines 22 and 36, respectively. Thus, fast-moving crews that can better isolate damage prior to intervention via heavily equipped (and slow-moving) RCs.

The timelines show that RCs operate manual switches after finishing their tasks, as they are already on site; this is in accordance with control center instructions. Post-repair manual switching is depicted by retaining RCs at the damage site for longer than the repair time, which is set to be two hours in this paper. In addition, battery discharging information at telecom APs is used in Case 3 to delay sending crews ($GC_{1,1}$, $GC_{2,1}$, $RC_{1,2}$, $RC_{2,2}$, $RC_{2,1}$, and $MC_{2,1}$) to their respective tasks, because opportunities for reconfiguration are blocked by the absence of the TS and are conducted only following the restoration of a portion of the TS at the 8th hour. This postponement of intervention allows another task to be assigned to the crew and avoids the cost of waiting at damage sites until TS recovery. Table II summarizes the availability of the TS for the full-overhead configuration in both Cases 2 and 3. The telecom-aware approach can restore the power supply to critical telecom points faster than can the telecom-agnostic approach (at the 8th hour), which accelerates later recovery operations.

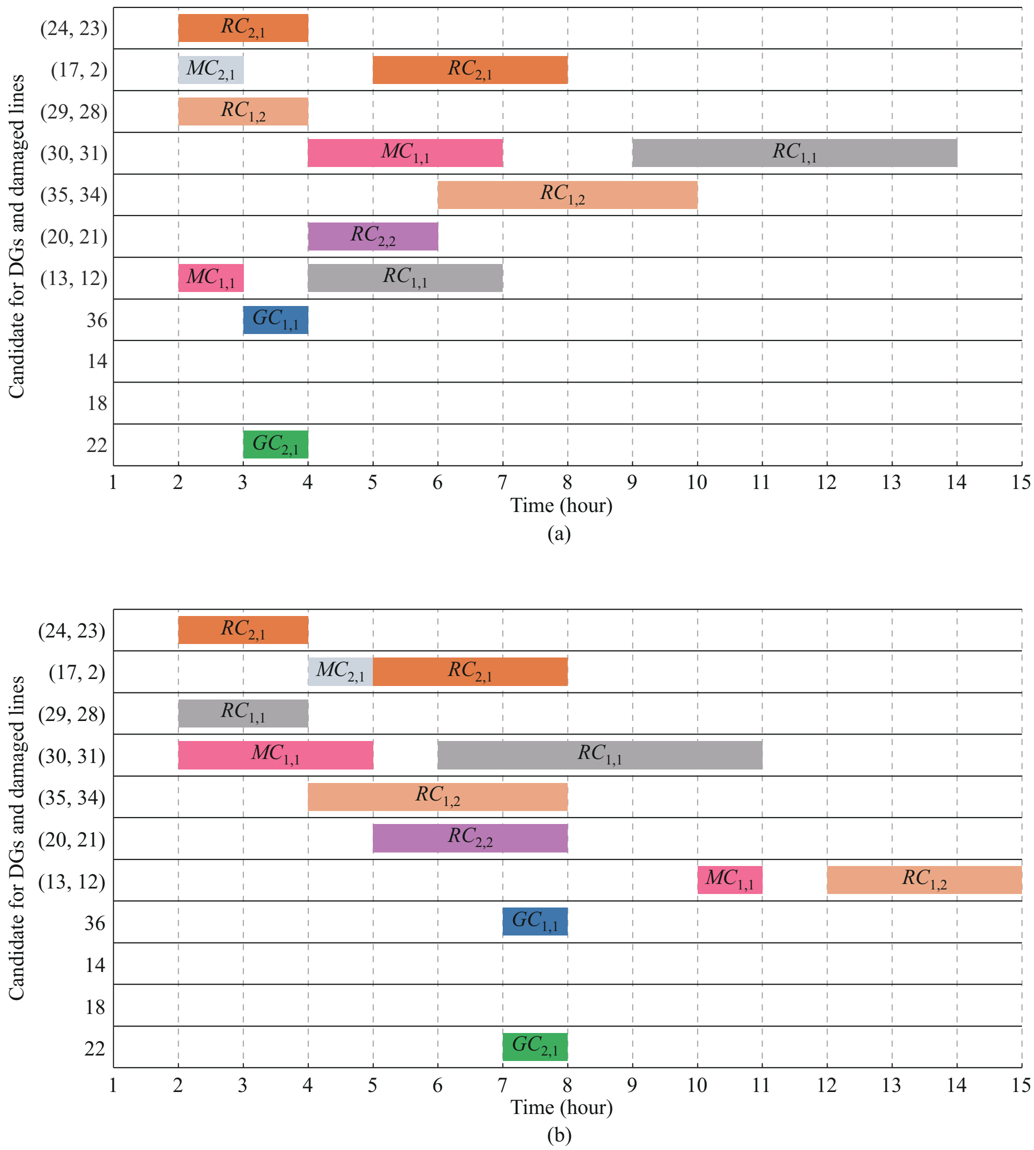

Fig. 5. Intervention crew schedules in Cases 2 and 3 for an overhead configuration. (a) Case 2. (b) Case 3.

TABLE II
AVAILABILITY OF TS FOR FULL-OVERHEAD CONFIGURATION

Case	Time (hour)	W_1, U_1, U_3, SS_2	X_2, W_2, U_2, SS_1, SS_3
2	0→2	TS up	TS up
	3→9	TS down	TS down
	10→13	TS up	TS down
	14→15	TS up	TS up
3	0→2	TS up	TS up
	3→7	TS down	TS down
	8→10	TS up	TS down
	11→15	TS up	TS up

Figure 6 shows the major steps in DSR for the full-overhead configuration in Case 3 based on the crew schedules presented in Fig. 5(b). The dashed and solid lines indicate open and closed lines, respectively, and the colored areas represent different zones of the power grid. Figure 6 can be briefly described as follows.

In Fig. 6(a), remote switches are operated during the fast response, where all damages are isolated and Buses 9, 10, and 11 are recovered by a feeder from SS_2, as their initial supply from SS_1 is interrupted. Due to the absence of a valid supply path, nodes 22 and 33 cannot be restored despite being distinguished from damaged zones.

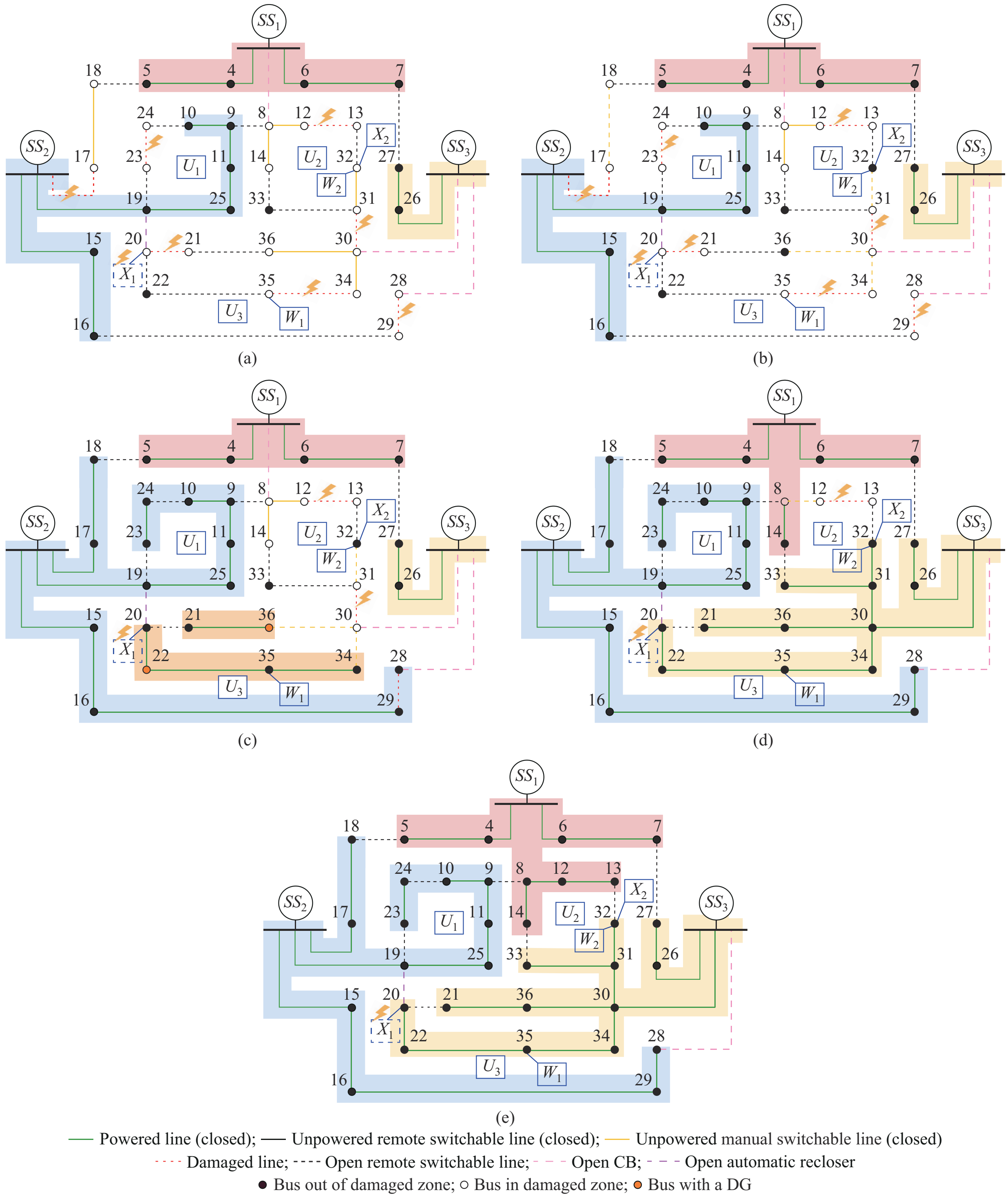

Fig. 6. Major steps in DSR for full-overhead configuration in Case 3. (a) Hours 0→4. (b) Hours 5→7. (c) Hours 8→10. (d) Hours 11→14. (e) Hour 15.

In Fig. 6(b), crews $MC_{1,1}$ and $MC_{2,1}$ complete their manual-switching tasks at the 5th hour, isolating damaged Lines 30-31 and 2-17, respectively. Note that repairs at Lines 23-24 and 28-29 are completed at the 4th hour. However, these lines cannot be reconnected because of the unavailability of TSs.

In Fig. 6(c), lines 20-21 and 34-35 are restored, enabling the installation of DGs at Buses 22 and 36 and the formation of two small microgrids (highlighted in orange). This in turn restores power to telecom point W_1, which enables many nodes to be recovered with the closing of remote switches at Lines 22-35 and 21-36. W_1 also allows Buses 17, 18, 23, 24, 28, and 29 to be restored following the repair of adjacent damage (previously Lines 23-24 and 28-29, and later Line 2-17).

In Fig. 6(d), damaged Line 30-31 is repaired, enabling telecom points X_2 and W_2 to be restored. This in turn allows multiple nodes to be reconnected to the main grid.

In Fig. 6(e), Line 12-13 is reconnected as soon as the repair is completed and TS is available.

B. DSR in 141- and 315-bus Systems

Two case studies with 141- and 315-bus systems are constructed from a real MV power grid to demonstrate the applicability of the proposed restoration approach to larger-scale power grids (27 and 59 MW load power, respectively). Unlike most systems in which manual switches are ignored and very few remote switches are analyzed, a switch (remote or manual) is considered at each line. A scenario of 10 failures is considered, where three depots host the restoration resources: $DP_1=\{RC_{1,1},RC_{1,2},MC_{1,1},GC_{1,1}\}$, $DP_2=\{RC_{2,1},RC_{2,2},MC_{2,1}\}$, $DP_3=\{RC_{3,1},MC_{3,1},GC_{3,1}\}$. For an overhead configuration, the DSR is solved in 225.3 and 267.4 s under the two 141-bus and 315-bus systems, respectively. The results presented in Fig. 7 confirm that Case 1 achieves the best restoration in terms of cumulative supplied power. Case 3 outperforms Case 2 following the same trend observed in Fig. 4, where the awareness of telecom point availability increases the potential of restoration. The problem is verified as NP-hard by combining a routing combinatorial optimization problem (with exponential complexity) and SDG operational constraints. The obtained results further confirm the validity of the proposed restoration approach and enable future studies to turn their focus to a solution with lower complexity.

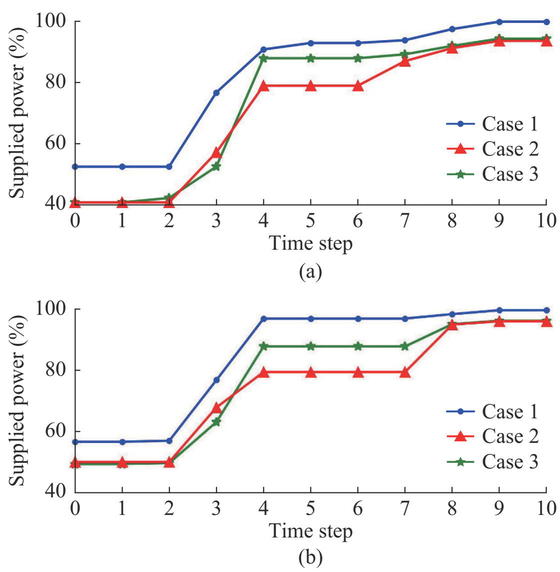

Fig. 7. Evolution of supplied power during DSR. (a) 141-bus system. (b) 315-bus system.

Finally, the main modeling contribution of this paper, which considers two-way power-telecom interdependencies in an SDG, is used in other practical applications such as new deployments of remote switches, crew sizing, and definitions of power-telecom service-level agreement (SLA) [35]. Accordingly, power-telecom interdependencies can be leveraged to improve the overall grid resilience through different existing applications. This insight can be extended to any industrial cyber-physical system in which the core functionality must be analyzed jointly with ICTs to achieve enhanced resilience.

IV. Conclusion

The restoration process in SDG is modeled by integrating power-telecom interdependencies and considering multiple resources. The reconfiguration of switches, RCs/MCs, and DGs is coordinated by means of a telecom-aware MILP co-optimization process, which yields improved resilience strategies. The advantages of tight damage isolation are revealed through an exploration of general cases of underground and overhead electrical networks. The proposed restoration approach incorporates both the contribution of communication networks to DSR (by connecting remote switches and field crews to central grid functions) and the power supply of telecom assets for a comprehensive analysis of bidirectional power-telecom interdependencies. The results of the case studies demonstrate that the co-optimization of resource allocation and telecommunications-aware strategic interventions enhances the DSR and improves the overall resilience of the grid. The application of the proposed restoration approach to real smart distribution grids validates its applicability.

Future studies will involve a more detailed model with increased accuracy for DGs, battery storage, load, and telecom dynamics. This is expected to increase the computational burden, which will necessitate the development of a lower-complexity solution algorithm.

References

[1] Z. Bie, Y. Lin, G. Li *et al*., "Battling the extreme: a study on the power system resilience," *Proceedings of the IEEE*, vol. 105, no. 7, pp. 1253-1266, Jul. 2017.

[2] Y. Wang, C. Chen, J. Wang *et al*., "Research on resilience of power systems under natural disasters–a review," *IEEE Transactions on Power Systems*, vol. 31, no. 2, pp. 1604-1613, Mar. 2016.

[3] Y. Liu, R. Fan, and V. Terzija, "Power system restoration: a literature review from 2006 to 2016," *Journal of Modern Power Systems and Clean Energy*, vol. 4, no. 3, pp. 332-341, May 2016.

[4] J. Liu, Y. Yu, and C. Qin, "Unified two-stage reconfiguration method for resilience enhancement of distribution systems," *IET Generation, Transmission & Distribution*, vol. 13, no. 9, pp. 1734-1745, May 2019.

[5] Q. Zhou, D. Shirmohammadi, W.-H. E. Liu, "Distribution feeder reconfiguration for service restoration and load balancing," *IEEE Transactions on Power Systems*, vol. 12, no. 2, pp. 724-729, May 1997.

[6] P. Van Hentenryck and C. Coffrin, "Transmission system repair and restoration," *Mathematical Programming*, vol. 151, no. 1, pp. 347-373, Mar. 2015.

[7] Y. P. Fang and G. Sansavini, "Optimum post-disruption restoration under uncertainty for enhancing critical infrastructure resilience," *Reliability Engineering & System Safety*, vol. 185, pp. 1-11, May 2019.

[8] G. Kandaperumal and A. K. Srivastava, "Resilience of the electric distribution systems: concepts, classification, assessment, challenges, and research needs," *IET Smart Grid*, vol. 3, no. 2, pp. 133-143, Apr. 2020.

[9] S. Poudel and A. Dubey, "A two-stage service restoration method for electric power distribution systems," *IET Smart Grid*, vol. 4, no. 5, pp. 500-521, Oct. 2021.

[10] N. Morshedlou, A. D. Gonzalex, and K. Barker, "Work crew routing problem for infrastructure network restoration," *Transportation Research Part B: Methodological*, vol. 118, pp. 66-89, Dec. 2018.

[11] R. Perez-Guerrero, G. T. Heydt, N. J. Jack *et al*., "Optimal restoration of distribution systems using dynamic programming," *IEEE Transactions on Power Delivery*, vol. 23, no. 3, pp. 1589-1596, Jul. 2008.

[12] C. Wang, P. Ju, S. Lei *et al*., "Markov decision process-based resilience enhancement for distribution systems: an approximate dynamic programming approach," *IEEE Transactions on Smart Grid*, vol. 11, no. 3, pp. 2498-2510, May 2020.

[13] M. M. Hosseini and M. Parvania, "Resilient operation of distribution grids using deep reinforcement learning," *IEEE Transactions on Industrial Informatics*, vol. 18, no. 3, pp. 2100-2109, Mar. 2022.

[14] A. Arif, Z. Wang, J. Wang *et al*., "Power distribution system outage management with co-optimization of repairs, reconfiguration, and DG

dispatch," *IEEE Transactions on Smart Grid*, vol. 9, no. 5, pp. 4109-4118, Sept. 2018.

[15] S. Lei, C. Chen, Y. Li *et al*., "Resilient disaster recovery logistics of distribution systems: co-optimize service restoration with repair crew and mobile power source dispatch," *IEEE Transactions on Smart Grid*, vol. 10, no. 6, pp. 6187-6202, Nov. 2019.

[16] Y. Bian, C. Chen, Y. Huang *et al*., "Service restoration for resilient distribution systems coordinated with damage assessment," *IEEE Transactions on Power Systems*, vol. 37, no. 5, pp. 3792-3804, Sept. 2022.

[17] W. Liu, Z. Lin, F. Wen *et al*., "A wide area monitoring system based load restoration method," *IEEE Transactions on Power Systems*, vol. 28, no. 2, pp. 2025-2034, May 2013.

[18] A. Ashok, M. Govindarasu, and J. Wang, "Cyber-physical attack-resilient wide-area monitoring, protection, and control for the power grid," *Proceedings of the IEEE*, vol. 105, no. 7, pp. 1389-1407, Jul. 2017.

[19] S. Xin, Q. Guo, H. Sun *et al*., "Information-energy flow computation and cyber-physical sensitivity analysis for power systems," *IEEE Journal on Emerging and Selected Topics in Circuits and Systems*, vol. 7, no. 2, pp. 329-341, Jun. 2017.

[20] G. Huang, J. Wang, C. Chen *et al*., "Cyber-constrained optimal power flow model for smart grid resilience enhancement," *IEEE Transactions on Smart Grid*, vol. 10, no. 5, pp. 5547-5555, Sept. 2019.

[21] Z. Ye, C. Chen, R. Liu *et al*., "Boost distribution system restoration with emergency communication vehicles considering cyber-physical interdependence," *IEEE Transactions on Smart Grid*, vol. 14, no. 2, pp. 1262-1275, Mar. 2023.

[22] X. Liu, B. Zhang, B. Chen *et al*., "Towards optimal and executable distribution grid restoration planning with a fine-grained power-communication interdependency model," *IEEE Transactions on Smart Grid*, vol. 13, no. 3, pp. 1911-1922, May 2022.

[23] X. Wang, Q. Kang, J. Gao *et al*., "Distribution network restoration supply method considers 5G base station energy storage participation," *Energy*, vol. 289, p. 129825, Feb. 2024.

[24] A. Kwasinski, W. W. Weaver, P. L. Chapman *et al.*, "Telecommunications power plant damage assessment for hurricane Katrina – site survey and follow-up results," *IEEE Systems Journal*, vol. 3, no. 3, pp. 277-287, Sept. 2009.

[25] S. A. Fenrick and L. Getachew, "Cost and reliability comparisons of underground and overhead power lines," *Utilities Policy*, vol. 20, no. 1, pp. 31-37, Mar. 2012.

[26] O. Al-Khatib, W. Hardjawana, and B. Vucetic, "Traffic modeling and optimization in public and private wireless access networks for smart grids," *IEEE Transactions on Smart Grid*, vol. 5, no. 4, pp. 1949-1960, Jul. 2014.

[27] E. Ancillotti, R. Bruno, and M. Conti, "The role of communication systems in smart grids: architectures, technical solutions and research challenges," *Computer Communications*, vol. 36, no. 17-18, pp. 1665-1697, Nov. 2013.

[28] Q. Yang, J. A. Barria, and T. C. Green, "Communication infrastructures for distributed control of power distribution networks," *IEEE Transactions on Industrial Informatics*, vol. 7, no. 2, pp. 316-327, May 2011.

[29] V. C. Gungor, D. Sahin, T. Kocak *et al*., "Smart grid technologies: communication technologies and standards," *IEEE Transactions on Industrial Informatics*, vol. 7, no. 4, pp. 529-539, Nov. 2011.

[30] M. Kuzlu, M. Pipattanasomporn, and S. Rahman, "Communication network requirements for major smart grid applications in HAN, NAN and WAN," *Computer Networks*, vol. 67, pp. 74-88, Jul. 2014.

[31] D. C. Paraskevopoulos, G. Laporte, P. P. Repoussis *et al*., "Resource constrained routing and scheduling: review and research prospects," *European Journal of Operational Research*, vol. 263, no. 3, pp. 737-754, Dec. 2017.

[32] U.S. Department of Energy, "Electric power telecommunications interdependencies," Tech. Rep., U.S. Department of Energy, 2023.

[33] *IEEE Guide for Smart Grid Interoperability of Energy Technology and Information Technology Operation with the Electric Power System (EPS), End-use Applications, and Loads*, IEEE Standard 2030-2011, 2011.

[34] *Management and Orchestration: Network and Services Operations for Energy Utilities*, 3GPP Specification 28.318, 2024.

[35] Y. N. Belaid, "Integrated power-telecom modeling for resilience quantification and optimization in smart distribution grids," Ph.D. dissertation, University of Paris-Saclay, Paris, France, Sept. 2023.

Youba Nait-Belaid received the B.Sc. degree in electrical engineering from the Institute of Electrical and Electronic Engineering, Boumerdes, Algeria, in 2016, and the M.Sc. degree in communications engineering and the Ph.D. in industrial engineering from CentraleSupélec, University of Paris-Saclay, Paris, France, in 2018 and 2023, respectively. He is currently a Postdoc Research Fellow at the Grid Integration Group, Lawrence Berkeley National Laboratory (LBNL), Berkeley Hills, USA. His research interests include smart grid, reliability, resilience, mathematical modeling, and optimization.

Yiping Fang received the Ph.D. degree in industrial engineering from École Centrale de Paris (ECP), Paris, France, in 2015, and was a Postdoc Research Fellow at ETH Zurich, Zurich, Switzerland, from 2015 to 2017. He is currently a Full Professor in the Chair Risk and Resilience of Complex Systems, Department of Industrial Engineering, CentraleSupélec, University of Paris-Saclay, Paris, France. His research interests include research and development of advanced computational methods for risk, reliability and resilience analytics of industrial system, and in particular, stochastic and robust optimization, risk and decision analysis, and reinforcement learning.

Zhiguo Zeng received the B.S. and Ph.D. degrees from Beihang University, Beijing, China, in 2011 and 2016, respectively. He is now a Full Professor at the Department of Industrial Engineering, CentraleSupélec, University of Paris-Saclay, Paris, France. His research interests include data-driven methods for reliability modeling, analysis and optimization, predictive maintenance, and resilience of complex system.

Patrick Coudray received the engineering degree from ENSTA, Paris, France, in 1990. He is currently working at Electricité de France (EDF) R&D, Paris, France, as a Research Engineer in the field of smart grid, contributing to many national and international projects. His research interest includes cross-resilience between telecommunications and power.

Anne Barros received the Ph.D. degree from University of Technology of Troyes, Troyes, France, in 2003, and then held a professorship position with the same university from 2003 to 2014. She was a Full-time Professor at Norwegian University of Science and Technology, Trondheim, Norway, from 2014 to 2019. She is currently a Professor in reliability and maintenance modelling at the Department of Industrial Engineering, CentraleSupélec, University of Paris-Saclay, Paris, France. She is currently heading the Risk, Reliability and Resilience (R3) Research Group and holding the Industrial Chair on Risk and Resilience of Complex Systems at CentraleSupélec, with the ambition to improve resilience assessment and maintenance modelling methods for complex systems. Her research interests include degradation modelling, prognostics, and condition-based and predictive maintenance.